Proper Motion and Natal Kick in the Galactic Black Hole X-Ray Binary AT2019wey

Downloaded from: https://research.chalmers.se, 2026-10-15 05:20 UTC

Citation for the original published paper (version of record):
Cui, L., Jiang, P., An, T. et al (2025). Proper Motion and Natal Kick in the Galactic Black Hole X-Ray Binary AT2019wey. Astrophysical Journal, 983(2).
http://dx.doi.org/10.3847/1538-4357/adc0f7

N.B. When citing this work, cite the original published paper.

research.chalmers.se offers the possibility of retrieving research publications produced at Chalmers University of Technology. It covers all kind of research output: articles, dissertations, conference papers, reports etc. since 2004. research.chalmers.se is administrated and maintained by Chalmers Library

(article starts on next page)

The Astrophysical Journal, 983:147 (6pp), 2025 April 20 https://doi.org/10.3847/1538-4357/adc0f7
© 2025. The Author(s). Published by the American Astronomical Society.
OPEN ACCESS

Proper Motion and Natal Kick in the Galactic Black Hole X-Ray Binary AT2019wey

Lang Cui[1,2,3], Pengfei Jiang[1], Tao An[4], Hongmin Cao[5], Ning Chang[1], Giulia Migliori[6], Marcello Giroletti[6], Sándor Frey[7,8,9], Jun Yang[10], Krisztina É. Gabányi[7,8,11,12], Xiaoyu Hong[4], and Wenda Zhang[13]
[1] Xinjiang Astronomical Observatory, CAS, 150 Science-1 Street, Urumqi 830011, People's Republic of China; cuilang@xao.ac.cn
[2] Key Laboratory of Radio Astronomy and Technology, CAS, A20 Datun Road, Chaoyang District, Beijing 100101, People's Republic of China
[3] Xinjiang Key Laboratory of Radio Astrophysics, 150 Science 1-Street, Urumqi 830011, People's Republic of China
[4] Shanghai Astronomical Observatory, CAS, 80 Nandan Road, Shanghai 200030, People's Republic of China
[5] School of Electronic and Electrical Engineering, Shangqiu Normal University, 298 Wenhua Road, Shangqiu, Henan 476000, People's Republic of China
[6] INAF—Istituto di Radioastronomia, Via Gobetti 101, 40129 Bologna, Italy
[7] Konkoly Observatory, HUN-REN Research Centre for Astronomy and Earth Sciences, Konkoly Thege Miklós út 15-17, H-1121 Budapest, Hungary
[8] CSFK, MTA Centre of Excellence, Konkoly Thege Miklós út 15-17, H-1121 Budapest, Hungary
[9] Institute of Physics and Astronomy, ELTE Eötvös Loránd University, Pázmány Péter sétány 1/A, H-1117 Budapest, Hungary
[10] Department of Space, Earth and Environment, Chalmers University of Technology, Onsala Space Observatory, 43992 Onsala, Sweden
[11] Department of Astronomy, Institute of Physics and Astronomy, ELTE Eötvös Loránd University, Pázmány Péter sétány 1/A, H-1117 Budapest, Hungary
[12] HUN-REN–ELTE Extragalactic Astrophysics Research Group, ELTE Eötvös Loránd University, Pázmány Péter sétány 1/A, H-1117 Budapest, Hungary
[13] National Astronomical Observatories, CAS, 20A Datun Road, Beijing 100012, People's Republic of China
Received 2024 April 28; revised 2025 March 13; accepted 2025 March 13; published 2025 April 16

Abstract

Understanding the formation mechanisms of stellar-mass black hole X-ray binaries (BHXBs) remains a fundamental challenge in astrophysics. The natal kick velocities imparted during black hole (BH) formation provide crucial constraints on these formation channels. In this work, we present a new-epoch very long baseline interferometry (VLBI) observation of the Galactic BHXB AT2019wey carried out in 2023. Combining with archival VLBI data from 2020, we successfully measure the proper motion of AT2019wey over a 3 yr timescale, namely, 0.78 ± 0.12 mas yr^{-1} in R.A. and -0.42 ± 0.07 mas yr^{-1} in decl. Employing the measured proper motion, we estimate its peculiar velocity and the potential kick velocity (PKV) through Monte Carlo simulations, incorporating uncertainties of its distance and radial velocity. The estimated PKV distributions and height above the Galactic plane suggest that AT2019wey's BH likely formed through a supernova explosion rather than direct collapse.

Unified Astronomy Thesaurus concepts: Stellar mass black holes (1611); X-ray binary stars (1811); Proper motions (1295); Very long baseline interferometry (1769)

1. Introduction

Black hole X-ray binaries (BHXBs) are binary systems consisting of a stellar-mass black hole (BH) accreting matter from a companion, typically a low-mass evolved star. BHXBs mostly remain in a quiescent state before transitioning into an outburst (R. A. Remillard & J. E. McClintock 2006). During these outbursts, BHXBs exhibit luminous X-ray emissions, but the compact radio jets are often quenched during the soft spectral state. Additionally, the accretion rate of BHs in BHXBs can fluctuate significantly over short timescales (R. Fender & T. Belloni 2012; R. Fender & E. Gallo 2014). BHXBs serve as critical astrophysical laboratories that enable us to study a wide range of phenomena related to accretion physics, jet formation, strong gravity effects around stellar-mass BHs, and binary evolution (A. A. Esin et al. 1997; J. E. McClintock & R. A. Remillard 2006; R. A. Remillard & J. E. McClintock 2006; R. P. Fender et al. 2009; R. J. H. Dunn et al. 2010; X. Liu et al. 2021; D. Ayzenberg & C. Bambi 2022; Q. Bu & S. Zhang 2023).

Variations in the accretion flow of BHXBs can significantly change the X-ray spectral energy distribution. The accretion states of BHXBs can be broadly classified into hard and soft states (e.g., R. Fender & T. Belloni 2004, 2012). Two distinct states of BHXBs correspond to different behaviors observed at radio wavelengths. The hard state is characterized by a continuous jet, while the soft state has never been observed to be associated with a quasi-steady jet (e.g., A. M. Stirling et al. 2001; D. M. Russell et al. 2011; R. Fender & E. Gallo 2014; J. S. Bright et al. 2020). Very long baseline interferometry (VLBI) is a powerful technique that provides the highest angular resolution for imaging the compact jets and structures in BHXBs (S. J. Tingay et al. 1995; I. F. Mirabel & L. F. Rodríguez 1999; A. M. Stirling et al. 2001; R. Fender & T. Belloni 2004; J. C. A. Miller-Jones 2008). It also enables precise astrometry and measurement of proper motions of BHXBs (e.g., J. C. A. Miller-Jones et al. 2009a, 2011; M. J. Reid et al. 2011, 2014a; P. Atri et al. 2020), providing insights into their formation mechanisms based on their space velocities (e.g., V. Dhawan et al. 2007; J. C. A. Miller-Jones et al. 2009b; P. Atri et al. 2019). The formation of a stellar-mass BH in these systems could occur either through supernovae (SNe) or through direct collapse (e.g., I. Mandel & B. Müller 2020; K. B. Burdge et al. 2024).

An example of such a system, which exhibits many of the remarkable properties of BHXBs, is AT2019wey, a newly identified Galactic microquasar hosting a candidate stellar-mass BH accretor. Since its initial detection as an optical transient in late 2019 by Asteroid Terrestrial-impact Last Alert System (J. Tonry et al. 2019) and subsequent association with an X-ray source (I. Mereminskiy et al. 2020), AT2019wey has been the subject of extensive multiwavelength campaigns from radio to X-rays (H. Cao et al. 2020; M. Giroletti et al. 2020; Y. Yao et al. 2020, 2021a, 2021b; N. Yadlapalli et al. 2021). These

Original content from this work may be used under the terms of the Creative Commons Attribution 4.0 licence. Any further distribution of this work must maintain attribution to the author(s) and the title of the work, journal citation and DOI.

observations, coupled with the detection of a persistent compact jet in VLBI imaging (Y. Yao et al. 2021b; H.-M. Cao et al. 2022), firmly established AT2019wey as a newly identified Galactic microquasar—a low-mass BHXB system exhibiting relativistic jets. Moreover, early VLBI studies of AT2019wey also resolved a flat-spectrum radio source on milliarcsecond scales and constrained a lower distance limit of >6 kpc based on the angular broadening imposed by interstellar scattering (N. Yadlapalli et al. 2021; H.-M. Cao et al. 2022). However, the relatively short VLBI epoch timelines (four epochs within an interval of ∼1 month) precluded a direct measurement of the system's proper motion during these initial VLBI observations.

In this work, we present a new-epoch VLBI observation made in 2023, allowing us to measure the proper motion of AT2019wey by combining with the 2020 observations over a 3 yr time baseline. These high-precision astrometric measurements allow us to probe the space velocity of this Galactic BHXB for the first time. Characterizing the jet properties and space motions is crucial for understanding accretion/ejection processes, binary evolution, and the formation of stellar-mass BHs. Measuring proper motions provides unique insights into the intrinsic velocities imparted by possible natal kicks during the SN explosion that created the BH. Our new VLBI observation of AT2019wey provides a unique opportunity to connect its proper motion to the BH's formation scenario and subsequent kinematic evolution in the Galactic environment.

2. VLBI Observation and Data Reduction

Three years after the last multiwavelength VLBI observations, we carried out again a ∼4 hr observation of AT2019wey at 4.926 GHz with the European VLBI Network (EVN) on 2023 October 4 (project code EC095). The radio telescopes Effelsberg (Germany), Jodrell Bank MKII (United Kingdom), Westerbork (The Netherlands), Medicina (Italy), Onsala (Sweden), Tianma (China), Toruń (Poland), and Irbene (Latvia) were involved in this project. The data were recorded at the rate of 2048 Mbps (8 × 32 MHz subbands, full polarization, two-bit sampling) and correlated in e-VLBI mode (A. Szomoru 2008). We utilized the phase-referencing technique to interleave scans between the phase-referencing calibrator J0442+5436 and the target AT2019wey (separated by 1.°3). The cycle time was 4 minutes, including 3 minutes for J0442+5436 and 1 minute for AT2019wey. A bright and compact source DA193 was inserted to be observed in the middle of these VLBI scans as a fringe finder.

We reduced the correlated data using the Astronomical Image Processing System (AIPS; E. W. Greisen 2003). First, we flagged data when the antennas were slewing or had other instrumental or recording problems. Parallactic angle and ionospheric corrections were then performed. A priori amplitude calibration was conducted with gain curves and system temperature measurements of each antenna. After manual phase calibrations on both DA193 and J0442+5436 to remove the instrumental delays, we performed the global fringe fitting on DA193 and J0442+5436, respectively. After that, imaging and self-calibrations in the DIFMAP software (M. C. Shepherd et al. 1994) were performed on the phase-referencing calibrator J0442+5436. Next, we performed the global fringe fitting in AIPS again using the obtained image of J0442+5436 as the input model to correct the phase errors caused by the structure of this calibrator. The phase and amplitude self-calibrations were also conducted with the obtained image of J0442+5436 in AIPS to reduce the residual phase and amplitude errors. Finally, we interpolated the derived solutions to the target AT2019wey in AIPS and imaged this target without self-calibration in DIFMAP.

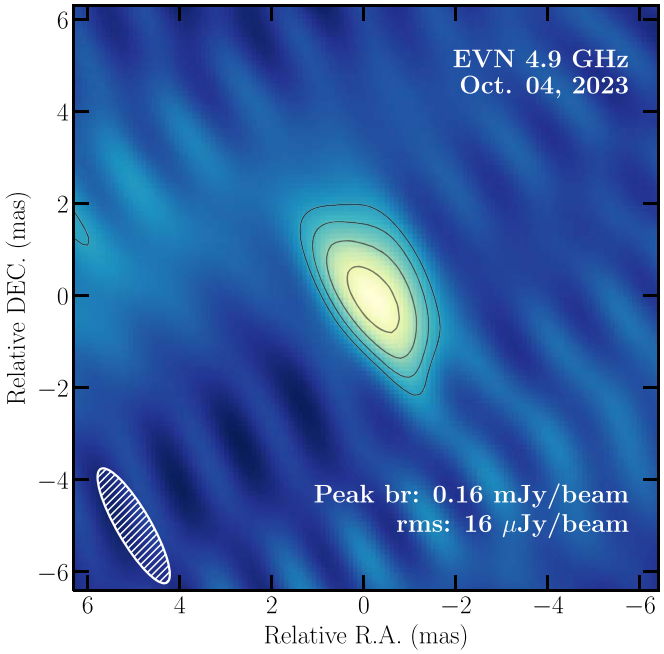

Figure 1. Naturally weighted image of AT2019wey obtained with the 4.9 GHz EVN observation on 2023 October 4. The peak brightness value and the image noise level are labeled in the lower-right corner. Contours start from 3σ noise level and increase by a factor of $\sqrt{2}$. The FWHM of the Gaussian synthesized beam is represented by an ellipse in the lower-left corner (2.86 × 0.73 mas^2, major axis position angle PA = 30.°2).

3. Results

3.1. The New VLBI Image

The naturally weighted image of AT2019wey obtained with the new EVN observation is presented in Figure 1. The source appears resolved in this image, as it is slightly wider than the elliptical model of the synthesized beam in the southeast–northwest direction. A fit to the calibrated visibility data with a circular Gaussian model gives a total flux density of 0.46 ± 0.16 mJy and a size of 1.6 ± 0.5 mas for this source. Here, we used the method provided by S.-S. Lee et al. (2008) to estimate the uncertainties of the flux density and source size. The fitted size is much larger than the theoretical minimum resolvable size (A. P. Lobanov 2005) of ∼0.4 mas in this naturally weighted image, confirming that the radio emission from AT2019wey is resolved in this observation.

H.-M. Cao et al. (2022) suggested that the resolved feature of AT2019wey on milliarcsecond scales could be explained as scatter broadening caused by the Galactic interstellar medium, based on its source angular size versus frequency trend. Compared with the results from H.-M. Cao et al. (2022), we found a good consistency between our fitted size (1.6 ± 0.5 mas at 4.9 GHz) and those derived from the previous two-epoch VLBA observations at a close observing frequency, namely, 2.0 ± 0.4 mas and 1.4 ± 0.3 mas at 4.5 GHz on 2020 November 24 and December 9, respectively. Given this, our new result could also support the hypothesis of scatter broadening.

3.2. Detection of Proper Motion

High precision in proper motion measurements is more easily achieved over a longer observing timeline, as proper motion is a time-dependent linear change in the source position. Based on multi-epoch VLBI observations spanning ∼2 months, H.-M. Cao et al. (2022) set an upper limit on the proper motion of AT2019wey: $\mu_\alpha < 3.8$ mas yr^{-1} and $\mu_\sigma < 0.9$ mas yr^{-1} in R.A. and decl., respectively. Combined with the new EVN observation, higher precision in proper motion measurements can be attained with a significantly extended observing span of ∼3 yr.

To determine the proper motion of AT2019wey, we measured the position of this source at each observation and analyzed the position errors. The AIPS task JMFIT was used to derive the peak position and the statistical uncertainty for images of each epoch. For phase-referencing observations, astrometric uncertainties are mainly caused by the ambiguity of station coordinates, Earth orientation, and troposphere errors. Based on the simulation of N. Pradel et al. (2006), we estimated that the astrometric uncertainties are ∼0.07 mas in R.A. and ∼0.08 mas in decl. for EVN observations, while ∼0.05 mas in R.A. and ∼0.08 mas in decl. for VLBA observations. Besides that, the astrometric errors caused by the residual unmodeled ionosphere cannot be neglected. Following an analytical calculation (M. J. Reid & M. Honma 2014; M. J. Rioja & R. Dodson 2020), our estimated error values are ∼0.07, ∼0.06, and ∼0.03 mas at 4.5, 4.9, and 6.7 GHz, respectively. Nevertheless, the position derived from the new EVN observation requires more comments. The participation of the Tianma telescope greatly improved the resolution along the southeast–northwest direction, yet it concurrently led to a poor (u, v) coverage, leaving a significant void for (u, v) radius at ∼30−110 Mλ (λ is the observing wavelength). The asymmetric resolved structure along the southeast–northwest direction and the possible artificial structure caused by the poor (u, v) coverage could make the measured reference point position change, resulting in astrometric errors for the proper motion fitting. Therefore, a more conservative error estimate for this position measurement should be provided. Given this, we measured the position of AT2019wey without Tianma data, and the differences between the position measurements are 0.34 mas in R.A. and 0.06 mas in decl. These are probably the largest potential position errors arising from the target source structure issues in this observation. For the phase-referencing calibrator J0442+5436, the same coordinates were used throughout all observations, thereby no additional error was propagated to the relative position measurements of the target source. We also examined the discrepancies in position when utilizing the structural model of the phase-referencing calibrator derived from different observing epochs for the new EVN observation, as the coverage of the (u, v) plane of the new observation is obviously different from the other observations. The error in the R.A. direction is at a negligible level of 0.01 mas, while in the decl. direction it is smaller than ∼0.1 mas. Finally, all errors are propagated to the source positions and summarized in Table 1.

We applied a least-squares linear regression on the position time series to fit the proper motion of AT2019wey. As shown in Figure 2, the measured proper motion is $\mu_\alpha = 0.78 \pm 0.12$ mas yr^{-1} and $\mu_\delta = -0.42 \pm 0.07$ mas yr^{-1}. The reduced χ^2 per degree of freedom of ∼0.9 is near unity, implying that the position errors are only slightly overestimated. Compared with the results from H.-M. Cao et al. (2022), our new values of proper motion fall well within the previous upper-limit range but provide more precise estimates.

3.3. Peculiar Velocity and Potential Kick Velocity

If a celestial body's position, distance, radial velocity, and proper motion are known, its peculiar velocity could also be estimated based on a model of Galactic rotation (e.g., M. J. Reid et al. 2009). In this paper, we provided the position and proper motion information for AT2019wey. For the distance of this source, Y. Yao et al. (2021a) set an upper limit of 10 kpc and H.-M. Cao et al. (2022) provided a lower limit of 6 kpc. However, the information on the radial velocity is lacking for this source. Here we estimate the expected radial velocity $v_{\rm rad}$ of AT2019wey assuming the system undergoing pure Galactic rotation around the Galactic center (e.g., P. Atri et al. 2019). We followed the calculation method from M. J. Reid et al. (2009), adopting solar motion parameters of ($U_\odot = 10.7 \pm 1.8$, $V_\odot = 15.6 \pm 6.8$, $W_\odot = 8.9 \pm 0.9$) km s^{-1} (M. J. Reid et al. 2014b) and a Galactic model where the Sun is assumed to be at 8 kpc from the Galactic center and the circular velocity is 220 km s^{-1} for a flat rotation curve (e.g., J. Bovy et al. 2012). At distances of [6, 8, 10] kpc, the derived radial velocities are [−43, −51, −57] km s^{-1}. With those derived radial velocities, the corresponding peculiar velocities are [27, 37, 46] km s^{-1}, respectively.

Furthermore, we estimate the potential kick velocity (PKV) for AT2019wey, which represents the peculiar velocity of the system when it crosses the Galactic plane (P. Atri et al. 2019). AT2019wey is not located precisely in the Galactic plane. Its galactic latitude of 5.°3 and a distance lower limit of 6 kpc (H.-M. Cao et al. 2022) imply that its height above the Galactic plane is greater than ∼550 pc. Given that the majority of star-forming regions reside within the Galactic plane, there is a high probability that AT2019wey was also formed within the plane. Note that there is still a possibility that the system could have been formed in, and ejected from, a globular cluster. Without better information on the age and nature of the donor, or about the radial velocity and distance and hence the exact orbit of the system, it is difficult to robustly rule out this possibility currently. In the case of being formed in the Galactic plane, AT2019wey is unlikely to be undergoing pure Galactic rotation about the Galactic center, since it should at least have some component of z-velocity (the velocity along the direction perpendicular to the Galactic plane), oscillating above and below the Galactic plane. In such an orbit, the peculiar velocity is not a conserved quantity. Hence PKV, the peculiar velocity of a system when it crosses the Galactic plane, serves as a more effective tool to comprehend the natal kick a BHXB received when the BH was born. Additionally, it should be noted that the estimated radial velocities do not accurately reflect the true radial velocity of the source, as it may have undergone kicks, thereby likely not adhering to a pure Galactic rotation about the Galactic center. Therefore, we adopted five possible Gaussian radial velocity distributions with medians of $v_{\rm rad}$, $v_{\rm rad} \pm 50$ km s^{-1}, and $v_{\rm rad} \pm 100$ km s^{-1} in the following calculations. Here we use the same code[14] reported in P. Atri et al. (2019), incorporating the Monte Carlo simulation technique to estimate the PKV probability distribution for AT2019wey. The PKV probability distributions of AT2019wey using five probable Gaussian

[14] https://github.com/pikkyatri/BHnatalkicks

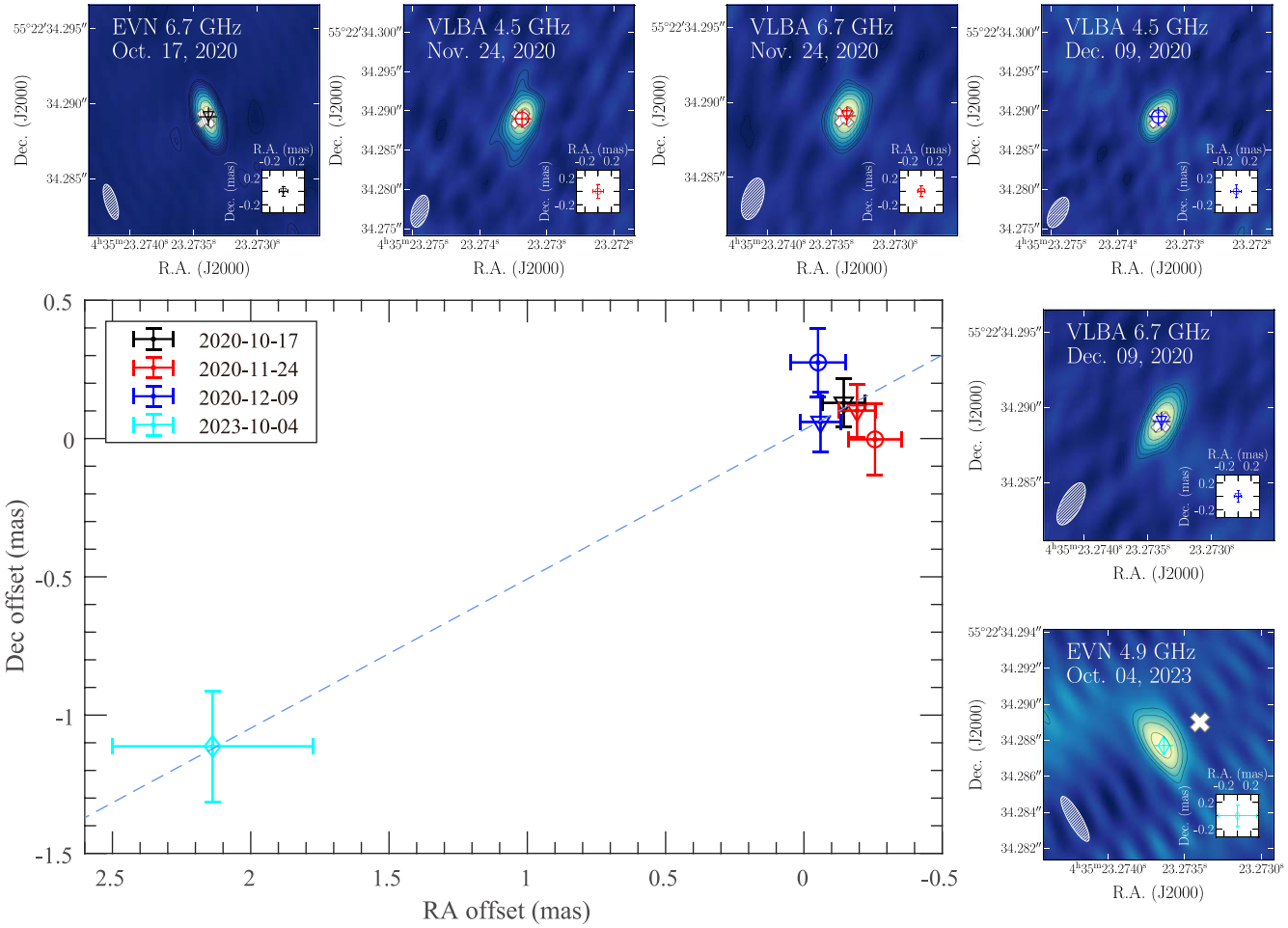

Figure 2. The sky position evolution of AT2019wey over 2020 to 2023 derived from multi-epoch VLBI observations is shown in the bottom-left panel. The blue dashed line represents the fitting proper motion. The surrounding panels are VLBI images of all epochs, while the colored markers represent the fitted positions listed in Table 1, with the error shown at the lower-right corner in each subfigure. The colors and shapes of the markers in the bottom-left panel indicate different observation epochs and frequencies: triangles represent 6.7 GHz, circles represent 4.5 GHz, and a diamond represents the new 4.9 GHz. The synthesized beam sizes are shown in the bottom-left corner of these panels.

Table 1
Phase-referenced Coordinates of AT2019wey Derived from JMFIT

Epoch	Obs. Data (y m d)	Frequency (GHz)	α (h m s)	$\sigma_{\alpha\cos\delta}$ (mas)	δ (d m s)	σ_δ (mas)
1	2020-10-17	6.7	04 35 23.273383	0.08	55 22 34.28913	0.09
2	2020-11-24	4.5	04 35 23.273370	0.10	55 22 34.28900	0.13
		6.7	04 35 23.273378	0.07	55 22 34.28910	0.10
3	2020-12-09	4.5	04 35 23.273394	0.10	55 22 34.28928	0.12
		6.7	04 35 23.273393	0.07	55 22 34.28906	0.11
4	2023-10-04	4.9	04 35 23.273651	0.36	55 22 34.28789	0.20

radial velocity distributions at three distances of [6, 8, 10] kpc are plotted in Figure 3, and their parameters are given in Table 2.

4. Discussion

The astrometric results derived from the EVN and VLBA observations spanning ∼3 yr show that AT2019wey has a significant proper motion. Based on the results, we estimate the peculiar velocity and PKV value of this source, which aid us in understanding the kick that the BHXB system received when the BH was born.

Given the distance uncertainty of this system and its unknown radial velocity, we provide the estimated peculiar velocity and the probability distributions of the PKV value under multiple scenarios in Section 3.3. With the assumption that the expected radial velocity is determined by the pure Galactic rotation at the Galactic longitude and distance of AT2019wey, and without considering its dispersion, the estimated peculiar velocity provides a relatively small value

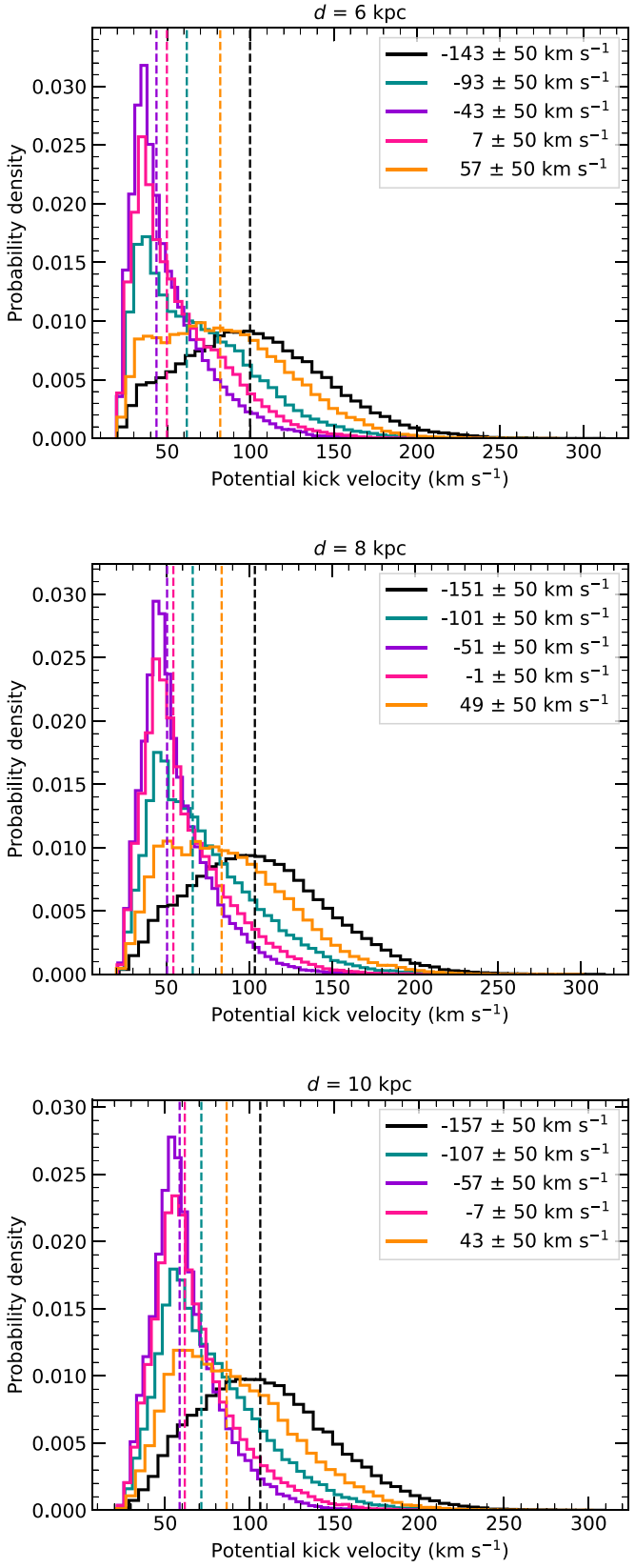

Figure 3. PKV probability distributions of AT2019wey using five probable Gaussian radial velocity distributions (noted in the legend of each panel) at three distances of [6, 8, 10] kpc. The vertical dashed lines represent the medians of the corresponding distributions. The parameters are listed in Table 2.

Table 2
PKV Probability Distribution of AT2019wey Using Five Probable Gaussian Radial Velocity Distributions at Three Distances of [6, 8, 10] kpc

d (kpc)	$v_{\rm rad}$ (km s^{-1})	PKV (km s^{-1})
6	-143 ± 50	100^{+78}_{-62}
	-93 ± 50	62^{+71}_{-34}
	-43 ± 50	44^{+54}_{-18}
	7 ± 50	50^{+62}_{-23}
	57 ± 50	82^{+72}_{-50}
8	-151 ± 50	103^{+76}_{-58}
	-101 ± 50	66^{+70}_{-32}
	-51 ± 50	51^{+48}_{-20}
	-1 ± 50	54^{+59}_{-22}
	49 ± 50	83^{+72}_{-45}
10	-157 ± 50	106^{+75}_{-55}
	-107 ± 50	71^{+66}_{-32}
	-57 ± 50	59^{+43}_{-23}
	-7 ± 50	62^{+55}_{-25}
	43 ± 50	86^{+71}_{-42}

Note. The PKV value given here represents the median of PKV probability distribution, with the lower and upper limits corresponding to the 5th and 95th percentiles, respectively.

relative to PKV. PKV, the peculiar velocity of a system at Galactic plane crossing, is a better proxy to investigate the BH natal kick. For a distance of 6 kpc and the central predicted radial velocity, the PKV probability distribution exhibits a significant positive skew, with a median value of $\sim$40 km s^{-1} and the highest probability density at $\sim$30 km s^{-1}. These values are lower than the typical velocity dispersion of stars in the Galaxy (50 km s^{-1}; F. Mignard 2000), which suggests that AT2019wey is likely to have formed either in an SN with a low natal kick or via direct collapse. However, the median PKV exceeds $\sim$50 km s^{-1} for the other four predicted radial velocities. Furthermore, all median PKV values fall within the range of $\sim$50–110 km s^{-1} for the distance of 8 and 10 kpc.

Based on three-dimensional (3D) SN simulations and semi-analytical parameterized models, I. Mandel & B. Müller (2020) developed a probabilistic model for natal kick velocities for neutron stars and BHs. For the latter, the probability distribution indicates that most BHs receive no natal kick at all, while the nonzero velocities can reach up to $\sim$150 km s^{-1}, with typical values around 60 km s^{-1}. Our estimated median PKV values of AT2019wey are consistent with this theoretical picture. Since BHXBs are more massive than common systems, they will suffer even lower velocity dispersions than that of common stars (50 km s^{-1}; F. Mignard 2000). In this case, these median PKV values fall within the range of $\sim$50–110 km s^{-1}, suggesting that AT2019wey is likely to be formed by an SN explosion rather than direct collapse.

The height of BHXB systems above the Galactic plane could be a supplementary proxy for the BH natal kick (e.g., P. G. Jonker & G. Nelemans 2004). The height above the Galactic plane for AT2019wey is greater than $\sim$550 pc. A similar situation is seen in many BHXB systems (the height greater than 500 pc) such as MAXI J1820+070, SAX J1819.3-2525, MAXI

J1836-194, GX 339-4, and 4U 1543-475, where their PKVs fall within the range of $\sim$60–240 km s^{-1}, suggesting that these systems have received a strong kick (P. Atri et al. 2019). Thus the height above the Galactic plane for AT2019wey also indicates that this system may have received a strong kick when the BH was born.

However, do note that the uncertainty in the distance of AT2019wey and its unknown radial velocity (especially the latter) make it extremely difficult to accurately estimate its PKV value, which in turn significantly complicates deducing its likely birth mechanism. Additionally, P. Nagarajan & K. El-Badry (2025) suggested that PKV is likely to overestimate the kick velocity, as it does not take into account the velocity dispersion of the local stellar population. For example, they found that MAXI J1820+070 needed a minimum kick of only 14 km s^{-1} and SAX J1819.3-2525 a minimum kick of only 44 km s^{-1}. P. Nagarajan & K. El-Badry (2025) argued that, after accounting for the stellar velocity dispersion, the kicks required for many of the known Galactic BHs seem to be overestimated in the literature. In our case, the distance of AT2019wey is uncertain, and thus a study similar to that of P. Nagarajan & K. El-Badry (2025) is not feasible at present to check if the kick for AT2019wey is also overestimated. Nevertheless, this underlines the difficulties and also the importance of accurate determination of natal kick velocities for Galactic BHs. We therefore encourage follow-up observations on AT2019wey to obtain more precise measurements or constraints on its distance and radial velocity, which are still crucial for fully reconstructing its 3D motion and formation history.

Acknowledgments

We thank the referee for the insightful and detailed comments that greatly helped us improve the manuscript. The European VLBI Network (EVN) is a joint facility of independent European, African, Asian, and North American radio astronomy institutes. Scientific results from data presented in this work are derived from the EVN project code: EC095. This work was supported by the CAS "Light of West China" Program (grant No. 2021-XBQNXZ-005) and the National SKA Program of China (grant No. 2022SKA0120102). L.C. acknowledges the support from the Tianshan Talent Training Program (grant No. 2023TSYCCX0099). T.A. and N.C. acknowledge the support from the Xinjiang Tianchi Talent Program. T.A. is supported by FAST Special Grant of NSFC (12041301). This work was also partly supported by the Urumqi Nanshan Astronomy and Deep Space Exploration Observation and Research Station of Xinjiang (XJYWZ2303). S.F. and K.É.G. thank the Hungarian National Research, Development and Innovation Office (NKFIH) for support (OTKA K134213). Their work was also supported by HUN-REN and the NKFIH excellence grant TKP2021-NKTA-64.

ORCID iDs

Lang Cui https://orcid.org/0000-0003-0721-5509
Pengfei Jiang https://orcid.org/0000-0003-3166-5657
Tao An https://orcid.org/0000-0003-4341-0029
Ning Chang https://orcid.org/0000-0002-8684-7303
Giulia Migliori https://orcid.org/0000-0003-0216-8053
Marcello Giroletti https://orcid.org/0000-0002-8657-8852
Sándor Frey https://orcid.org/0000-0003-3079-1889
Jun Yang https://orcid.org/0000-0002-2322-5232
Krisztina É. Gabányi https://orcid.org/0000-0003-1020-1597

References

Atri, P., Miller-Jones, J. C. A., Bahramian, A., et al. 2019, MNRAS, 489, 3116
Atri, P., Miller-Jones, J. C. A., Bahramian, A., et al. 2020, MNRAS, 493, L81
Ayzenberg, D., & Bambi, C. 2022, in Handbook of X-ray and Gamma-ray Astrophysics, ed. C. Bambi & A. Santangelo (Singapore: Springer), 81
Bovy, J., Allende Prieto, C., Beers, T. C., et al. 2012, ApJ, 759, 131
Bright, J. S., Fender, R. P., Motta, S. E., et al. 2020, NatAs, 4, 697
Bu, Q., & Zhang, S. 2023, in Handbook of X-ray and Gamma-ray Astrophysics, ed. C. Bambi & A. Santangelo (Singapore: Springer), 139
Burdge, K. B., EI-Badry, K., Kara, E., et al. 2024, Nature, 635, 316
Cao, H., Frey, S., Gabanyi, K., et al. 2020, ATel, 13984, 1
Cao, H.-M., Migliori, G., Giroletti, M., et al. 2022, A&A, 657, A104
Dhawan, V., Mirabel, I. F., Ribó, M., & Rodrigues, I. 2007, ApJ, 668, 430
Dunn, R. J. H., Fender, R. P., Körding, E. G., Belloni, T., & Cabanac, C. 2010, MNRAS, 403, 61
Esin, A. A., McClintock, J. E., & Narayan, R. 1997, ApJ, 489, 865
Fender, R., & Belloni, T. 2004, ARA&A, 42, 317
Fender, R., & Belloni, T. 2012, Sci, 337, 540
Fender, R., & Gallo, E. 2014, SSRv, 183, 323
Fender, R. P., Homan, J., & Belloni, T. M. 2009, MNRAS, 396, 1370
Giroletti, M., Cao, H., An, T., et al. 2020, ATel, 14168, 1
Greisen, E. W. 2003, in Information Handling in Astronomy—Historical Vistas, ed. A. Heck (Dordrecht: Springer), 109
Jonker, P. G., & Nelemans, G. 2004, MNRAS, 354, 355
Lee, S.-S., Lobanov, A. P., Krichbaum, T. P., et al. 2008, AJ, 136, 159
Liu, X., Chang, N., Wang, X., & Yuan, Q. 2021, Galax, 9, 78
Lobanov, A. P. 2005, arXiv:astro-ph/0503225
Mandel, I., & Müller, B. 2020, MNRAS, 499, 3214
McClintock, J. E., & Remillard, R. A. 2006, in Compact Stellar X-ray Sources, ed. W. Lewin & M. van der Klis, Vol. 39 (Cambridge: Cambridge Univ. Press), 157
Mereminskiy, I., Medvedev, P., Semena, A., et al. 2020, ATel, 13571, 1
Mignard, F. 2000, A&A, 354, 522
Miller-Jones, J. C. A. 2008, JPhCS, 131, 012057
Miller-Jones, J. C. A., Jonker, P. G., Dhawan, V., et al. 2009a, ApJL, 706, L230
Miller-Jones, J. C. A., Jonker, P. G., Nelemans, G., et al. 2009b, MNRAS, 394, 1440
Miller-Jones, J. C. A., Jonker, P. G., Ratti, E. M., et al. 2011, MNRAS, 415, 306
Mirabel, I. F., & Rodríguez, L. F. 1999, ARA&A, 37, 409
Nagarajan, P., & El-Badry, K. 2025, PASP, 137, 034203
Pradel, N., Charlot, P., & Lestrade, J. F. 2006, A&A, 452, 1099
Reid, M. J., & Honma, M. 2014, ARA&A, 52, 339
Reid, M. J., McClintock, J. E., Narayan, R., et al. 2011, ApJ, 742, 83
Reid, M. J., McClintock, J. E., Steiner, J. F., et al. 2014a, ApJ, 796, 2
Reid, M. J., Menten, K. M., Brunthaler, A., et al. 2014b, ApJ, 783, 130
Reid, M. J., Menten, K. M., Zheng, X. W., et al. 2009, ApJ, 700, 137
Remillard, R. A., & McClintock, J. E. 2006, ARA&A, 44, 49
Rioja, M. J., & Dodson, R. 2020, A&ARv, 28, 6
Russell, D. M., Miller-Jones, J. C. A., Maccarone, T. J., et al. 2011, ApJL, 739, L19
Shepherd, M. C., Pearson, T. J., & Taylor, G. B. 1994, BAAS, 26, 987
Stirling, A. M., Spencer, R. E., de la Force, C. J., et al. 2001, MNRAS, 327, 1273
Szomoru, A. 2008, in Proc. 9th European VLBI Network Symp. on The role of VLBI in the Golden Age for Radio Astronomy and EVN Users Meeting (IX EVN Symposium) (Trieste: SISSA), 40
Tingay, S. J., Jauncey, D. L., Preston, R. A., et al. 1995, Natur, 374, 141
Tonry, J., Denneau, L., Heinze, A., et al. 2019, TNSTR, 2019-3, 1
Yadlapalli, N., Ravi, V., Yao, Y., Kulkarni, S. R., & Brisken, W. 2021, ApJL, 909, L27
Yao, Y., Enoto, T., Altamirano, D., et al. 2020, ATel, 13932, 1
Yao, Y., Kulkarni, S. R., Burdge, K. B., et al. 2021a, ApJ, 920, 120
Yao, Y., Kulkarni, S. R., Gendreau, K. C., et al. 2021b, ApJ, 920, 121